

Response of tropospheric water vapor and temperature to El Niño warming in four NCAR models

Tao Zhang and De-Zheng Sun

**CIRES/Climate Diagnostics Center
&NOAA/Earth System Research Laboratory
Boulder, Colorado**

E-mail: tao.zhang@noaa.gov

November 1, 2006

(Submitted to *Geophys. Res. Lett.*)

Abstract

To diagnose the causes of an excessive response of the clear-sky greenhouse effect to El Niño warming in the NCAR models, the response of both water vapor and temperature to El Niño warming in the models is examined as a function of height. The percentage response of water vapor to El Niño warming in the models is considerably stronger than the response in the NCEP reanalysis in the middle and upper troposphere (700mb-300mb). The maximum discrepancy with NCEP data at 500 mb reaches 18%/K in CAM3 at T42 and T85 resolution. The discrepancy in the temperature response between the models and NCEP data at all tropospheric levels is within 0.3 K/K, with the maximum discrepancy occurring in the immediate neighborhood of 600 mb.

Employing a radiative model, we have calculated the contributions of the excessive water vapor response in the middle and upper troposphere as well as the contributions from the differences in the lapse rate response to the discrepancies seen in the clear-sky greenhouse effect. The results confirm that the main cause of the excessive response of the clear-sky greenhouse effect is an excessive response of water vapor in the middle and upper troposphere.

1. Introduction

Water vapor is the major contributor to Earth's greenhouse effect (Kiehl and Trenberth 1997). The response of the climate system to an increase in the greenhouse gases depends on the feedback of water vapor (Houghton et al. 2001). As we increasingly rely on climate models to assess and predict climate change, we need to know how well our models simulate the water vapor feedback (Stocker et al. 2001, Sun et al. 2001).

The response of water vapor to El Niño warming stands as a useful test bed to isolate and fix potential errors in our simulations of water vapor feedback. This is because the signal is strong, planetary in spatial scale, and has a time scale on which we have good observations. Earlier studies have stressed that El Niño warming is not a good surrogate for global warming because the latter may have a different spatial pattern of warming (Sun and Held 1996 and others). This argument has given back some ground recently as more and more climate models predict El Niño-like warming in response to increases in the greenhouse gases (Meehl and Washington 1996; Timmerman et al. 1999; Cai and Whetton 2000; Boer et al. 2004). Exactly how the climate system responds to anthropogenic forcing may take some time to answer. Fortunately, the need to document carefully and understand the discrepancies between model simulated response of the greenhouse effect of water vapor and that indicated in available observations does not depend much on the answer to this question.

In an earlier study of water vapor feedback in the NCAR CCM3, Sun et al. (2003) found that the response of the clear-sky greenhouse effect to El Niño warming in the model is considerably larger than that indicated in the ERBE observations. In an extended study by Sun et al. (2006), they found that three recent versions of the NCAR Community Atmosphere Model (CAM) continue to overestimate the response of clear-sky greenhouse effect to El Niño warming.

The clear-sky greenhouse effect depends on the water vapor (Zhang and Sun 2006) as well as on the lapse rate (Sun and Lindzen 1993; Held and Soden 2000). Therefore there are two possible causes of the excessive response in the clear-sky greenhouse effect. One is that the response of the water vapor concentration in the troposphere is too strong in the model. The other possibility is that the lapse rate response in the models is not the same as in the observations. We would like to know the relative contributions from these two processes to the excessive response in the clear-sky greenhouse effect noted in the NCAR models. Therefore we examine in this paper the vertical structure of both the water vapor and temperature response to El Niño warming, and we will quantify the contributions from these two factors to the discrepancies seen in the response of the clear-sky greenhouse effect.

2. Methodology, data and model

We employ the same regression analysis of Zhang and Sun (2006) in this study. As we attempt to understand the discrepancy in the clear-sky greenhouse effect between those in the models and that from ERBE (Barkstrom 1984), we again focus on the ERBE period.

The specific humidity and air temperature data from the National Centers for Environmental Prediction-National Center for Atmospheric Research (NCEP-NCAR) reanalysis (Kalnay et al. 1996) are used to examine the model simulations in the present study. The four NCAR models analyzed here are NCAR CCM3, NCAR CAM2, NCAR CAM3 at standard resolution, and NCAR CAM3 at T85. The model data are from the AMIP (Atmospheric Model Intercomparison Project) runs of the four models (Gates 1992).

3. Results

Figure 1 shows the spatial pattern of the response of clear-sky greenhouse effect (G_a) in ERBE observations and in the models. All the models can simulate the observed positive response from the greenhouse effect of water vapor including the location of the maximum response over the central Pacific, but somewhat overestimate the magnitude of the response. Averaged over the immediate region of El Niño warming (160°E - 290°E , 5°S - 5°N), the response of greenhouse effect is $6.37 \text{ Wm}^{-2}\text{K}^{-1}$ in ERBE observations while the response of G_a in four models is respectively $8.26 \text{ Wm}^{-2}\text{K}^{-1}$ (CAM1), $8.17 \text{ Wm}^{-2}\text{K}^{-1}$

(CAM2), $8.33 \text{ Wm}^{-2}\text{K}^{-1}$ (T42 CAM3) and $8.65 \text{ Wm}^{-2}\text{K}^{-1}$ (T85 CAM3). So all the models have an excessive response in Ga over the immediate region of El Niño warming and this excessive response is more severe in the T85 CAM3.

The differences in the response of greenhouse effect between the model simulations and ERBE observations could be in part due to the sampling differences between ERBE and the model data (Sun et al. 2006), but the bias due to the inadequate sampling does not explain the large range in the discrepancy as argued by Sun et al. (2006). Note that these values presented here are the results of regional response. An early study of Soden (1997) concluded that the response of the tropical mean greenhouse effect of water vapor to El Niño warming in the GFDL model has a close match with that from ERBE observations. We have to note, however, that the tropical mean signal of Ga associated with ENSO is much weaker than the signal averaged over the equatorial cold-tongue region of concern due to cancellations between different regions. The mean response of Ga averaged over the entire domain (120°E - 290°E , 30°S - 30°N) is respectively $0.79 \text{ Wm}^{-2}\text{K}^{-1}$ for observations, $1.04 \text{ Wm}^{-2}\text{K}^{-1}$ for CAM1, $0.77 \text{ Wm}^{-2}\text{K}^{-1}$ for CAM2, $1.00 \text{ Wm}^{-2}\text{K}^{-1}$ for CAM3 at T42, and $1.17 \text{ Wm}^{-2}\text{K}^{-1}$ for CAM3 at T85 resolution. So only over the region of immediate warming, all the models overestimate the response of Ga, and the cause of this overestimate is our concern here. The differences in the drying region will be investigated in a separate paper.

Figure 2 shows the percentage water vapor response at different levels of the troposphere, averaged over the immediate region of El Niño warming (160°E-290°E, 5°S-5°N). In both models and observations, the response increases with height to about 500-400 mb, then decreases with height further up. (Note that NCEP has no data above 300 mb, so only the response below this level is plotted). The model-data discrepancy in the response of water vapor is small in the low troposphere, but large differences occur in the middle and upper troposphere.

Figure 3 further shows a comparison of the vertical profile of the temperature response between the NCEP reanalysis and the models. The discrepancy in the temperature response between models and NCEP data at all tropospheric levels is within 0.3 K/K. The maximum discrepancy in the temperature response occurs in the immediate neighborhood of 600 mb. The response of temperature in the middle troposphere is weaker in the models than that from NCEP reanalysis. The cause for this underestimate in the middle troposphere is that the cold phase is generally warmer in the models than in the observations (not shown here).

To obtain a quantitative measure of the relative contributions to the errors in the clear-sky greenhouse effect from the bias in the response of temperature and the bias in the response of water vapor, we have employed a radiation model (Chou 1986), the same radiation routine used in Sun and Lindzen (1993) to calculate the differences in the greenhouse effect due to different temperature or water vapor profiles. To estimate the

contributions from the differences in the lapse rate response to the differences in the clear-sky greenhouse effect response, we first use the annual mean vertical profile of water vapor and temperature from NCEP reanalysis to calculate the mean clear-sky greenhouse effect as a reference value of G_a . We then add to the reference profiles of temperature the temperature response from NCEP data and models shown in Fig.3, for a 1 K increase in the SST. We keep the water vapor profile fixed unchanged in the calculation of G_a . We then contrast the differences between G_a from the changed temperature profile and G_a from the case with the reference temperature profile. Similarly, to estimate the contributions from the differences in the water vapor response to the differences in the clear-sky greenhouse effect, we keep the temperature profile fixed to the reference profile, but add to the reference profile for water vapor the response of water vapor for a 1 K increase in the SST (Fig.2). To quantify the combined contributions from the differences in the water vapor response and the differences in the temperature response to the differences in the response of G_a , we add to both profiles of water vapor and temperature their corresponding changes for a 1 K increase in the SST as shown in Fig. 2 and Fig. 3. The results from these calculations are summarized in Table 1. Clearly, the differences in the water vapor response explain the bulk of the differences in the response of G_a . The contribution from the differences in the temperature response is secondary. Note that the discrepancies in G_a do not exactly match the contributions due to the combined effect. This is expected because in our calculation, we have fixed the humidity above 300 mb constant—we do not have data from NCEP above this level.

4. Summary

To understand the causes of the overestimate in the response of clear-sky greenhouse effect to El Niño warming over the region of warming in four NCAR models, the response of water vapor and temperature to El Niño warming is examined as a function of height. Consistent with the results from the NCEP reanalysis, all the NCAR models have a stronger water vapor response to the surface ocean warming in the middle to upper troposphere than in the lower troposphere. However, the water vapor response in the middle to upper troposphere in the models is considerably stronger than in the NCEP reanalysis. The temperature response, in contrast is weaker in the models in the middle troposphere (the level around 600 mb).

Utilizing a radiation model, the data-model discrepancy in the temperature response is found to play a secondary role in giving rise to the bias of greenhouse effect. The difference in the temperature response only accounts for about 10% of the bias in the response of greenhouse effect. The overestimate in the response of greenhouse effect is mostly due to an overestimate of the response in the middle to upper tropospheric water vapor.

Consistent with earlier analysis (Sun et al. 2001), the correlation between the upper tropospheric humidity variations and those at the surface level is found to be higher in the NCAR models than in the observations. Therefore a possible excessive background diffusion in the models continues to be a concern. Another possible cause of the

overestimate of the water vapor response is the excessive response in the cloud cover. We have noted that all the models also overestimate the upper cloud cover response. The overestimate of water vapor response in the upper troposphere is about 8%/K ~10%/K, and the associated upper cloud cover response is overestimated by about 5%/K in CCM3 and about 3%/K in three latest versions (see Table 2 of Zhang and Sun (2006)). In the middle troposphere, two CAM3 models have a comparable cloud response to El Niño warming but they have an excessive water vapor response (the overestimate is about 20%/K). Interestingly, for other two models, the water vapor response is also considerably larger in the middle troposphere but the middle cloud response is apparently underestimated. This again highlights the fact that we do not yet know well the relationship between clouds and humidity, and more generally the precipitation efficiency of tropical convection. With new satellite data from "A Train" (Stephens et al. 2002), we may be in a better position to address these critical climate issues.

Acknowledgement

This research was supported by NOAA's Climate Dynamics and Environmental Prediction Program, and by NSF's climate dynamics program under ATM-9912434, ATM-0332760, and ATM 0553111. The authors would like to thank Dr. James J. Hack and Dr. Jeff Kiehl of NCAR for providing us the outputs from T85 CAM3.

References

- Barkstrom, B. R. , 1984: The Earth Radiation Budget Experiment (ERBE), *Bull. Am. Meteorol. Soc.*, **65**, 1170–1185.
- Boer G. J., B. Yu, S.-J. Kim, and G. M. Flato, 2004: Is there observational support for an El Niño-like pattern of future global warming? *Geophys. Res. Lett.*, **31**, L06201, doi:10.1029/2003GL018722.
- Cai W., and P. H. Whetton, 2000: Evidence for a time-varying pattern of greenhouse warming in the Pacific Ocean. *Geophys. Res. Lett.*, **27**, 2577–2580.
- Chou, M. D., 1986: Atmospheric solar heating rate in water vapour bands. *J. Climate Appl. Meteor.*, **25**, 1532-1542.
- Gates, W. L., 1992: AMIP: The Atmospheric Model Intercomparison Project. *Bull. Amer. Meteor. Soc.*, **73**, 791–794.
- Held, I. M. and B. J. Soden, 2000: Water vapor feedback and global warming. *Ann. Rev. Energy Environ.*, **25**, 441-475.
- Houghton J. T., Y. Ding, D. J. Griggs, M. Noguer, P. J. van der Linden, X. Dai, K. Maskell, and C. A. Johnson, 2001: *Climate Change 2001: The Scientific Basis*. Cambridge University Press, 881 pp.
- Kiehl, J. T., and K. E. Trenberth, 1997: Earth’s annual global mean energy budget. *Bull. Amer. Meteor. Soc.*, **78**, 197–208.
- Kalnay, E., and Coauthors, 1996: The NCEP/NCAR 40-Year Reanalysis Project. *Bull. Amer. Meteor. Soc.*, **77**, 437–471.
- Meehl G. A., and W. M. Washington, 1996: El Niño-like climate change in a model with increased atmospheric CO₂ concentrations. *Nature*, **382**, 56–60.
- Soden, B. J., 1997: Variations in the tropical greenhouse effect during El Niño, *J. Clim.*, **10**, 1050–1055.
- Stephens G. L, Coauthors, 2002: The Cloudsat Mission and the A-Train. *Bull. Amer. Meteor. Soc.*, **83**, 1771–1790.

Stocker, T. F., and Coauthors, 2001: Physical climate processes and feedbacks. *Climate Change 2001: The Scientific Basis* (Contribution of Working Group I to the Third Assessment Report of the Intergovernmental Panel on Climate Change). J. T. Houghton et al., Eds., Cambridge University Press, 417-470.

Sun, D.-Z., and R. S. Lindzen, 1993: Water vapor feedback and the ice age snowline record. *Ann. Geophys.*, **11**, 204-215.

Sun D.-Z., and I. Held, 1996: A comparison of modeled and observed relationships between interannual variations of water vapor and temperature. *J. Climate*, **9**, 665–675.

Sun, D.-Z., C. Covey, and R. S. Lindzen, 2001: Vertical correlations of water vapor in GCMs, *Geophys. Res. Lett.*, **28**, 259–262.

Sun, D.-Z., J. Fasullo, T. Zhang, and A. Roubicek, 2003: On the radiative and dynamical feedbacks over the equatorial cold-tongue. *J. Clim.*, **16**, 2425-2432.

Sun, D.-Z., T. Zhang, C. Covey, S. A. Klein, W. D. Collins, J. J. Hack, J. T. Kiehl, G. A. Meehl, I. M. Held, and M. Suarez, 2006: Radiative and Dynamical Feedbacks Over the Equatorial Cold-tongue: Results from Nine Atmospheric GCMs. *J. Clim.*, **19**, 4059-4074.

Timmerman A. J., J. Oberhuber, A. Bacher, M. Esch, M. Latif, and E. Roeckner, 1999: Increased El Niño frequency in a climate model forced by future global warming. *Nature*, **398**, 694–696.

Zhang, T. and D.-Z. Sun, 2006: Response of water vapor and clouds to El Niño warming in three National Center for Atmospheric Research atmospheric Models. *J. Geophys. Res.*, **111**, D17103, doi:10.1029/2005JD006700.

Table captions

Table 1: The discrepancy with ERBE observations in the response of clear-sky greenhouse effect (Ga) and the contributions to this discrepancy due to the errors in temperature and humidity response in NCAR models over the region of El Niño warming (160°E-290°E, 5°S-5°N). The contributions to Ga discrepancy are calculated as the differences in the response of Ga to 1K SST increase between models and the same NCEP reference value for each case (see text for details).

Figure captions

Figure 1: Response of the greenhouse effect of water vapor (Ga) to El Niño warming from (a) ERBE observations, (b) CAM1, (c) CAM2, (d) T42 CAM3, and (e) T85 CAM3. Shown are regression coefficients obtained by linearly regressing the greenhouse effect of water vapor at each grid point against the underlying SST averaged over the region of El Niño warming (160°E-290°E, 5°S-5°N). The interannual variations of Ga over the ERBE period are used for the calculations.

Figure 2: Percentage response of specific humidity to El Niño warming as a function of height from the NCEP-NCAR reanalysis and four NCAR models averaged over the

equatorial Pacific (160°E - 290°E , 5°S - 5°N). Shown are regression coefficients divided by the respective climatology. In every vertical level, the regression coefficients are obtained by linearly regressing specific humidity at the corresponding level against the underlying SST (as in Figure 19 of Zhang and Sun [2006]) averaged over the region of El Niño warming (160°E - 290°E , 5°S - 5°N). The interannual variations of specific humidity over the ERBE period are used for the regression calculations.

Figure 3: Response of air temperature to El Niño warming as a function of height from the NCEP-NCAR reanalysis and four NCAR models averaged over the equatorial Pacific (160°E - 290°E , 5°S - 5°N). Shown in every vertical level are regression coefficients obtained by linearly regressing the air temperature at the corresponding level against the underlying SST averaged over the region of El Niño warming (160°E - 290°E , 5°S - 5°N). The interannual variations of air temperature over the ERBE period are used for the regression calculations.

Model	Ga discrepancy with ERBE	contribution to the discrepancy ($\text{Wm}^{-2}\text{K}^{-1}$)		
Names	observations ($\text{Wm}^{-2}\text{K}^{-1}$)	Lapse rate effect	Humidity effect	combined effect
CAM1	1.89	0.053	1.65	1.71
CAM2	1.80	0.31	0.87	1.21
CAM3	1.96	0.23	1.12	1.39
CAM3 (T85)	2.28	0.020	1.66	1.70

Table 1: The discrepancy with ERBE observations in the response of clear-sky greenhouse effect (Ga) and the contributions to this discrepancy due to the errors in temperature and humidity response in NCAR models over the region of El Niño warming (160°E - 290°E , 5°S - 5°N). The contributions to Ga discrepancy are calculated as the differences in the response of Ga to 1K SST increase between models and the same NCEP reference value for each case (see text for details).

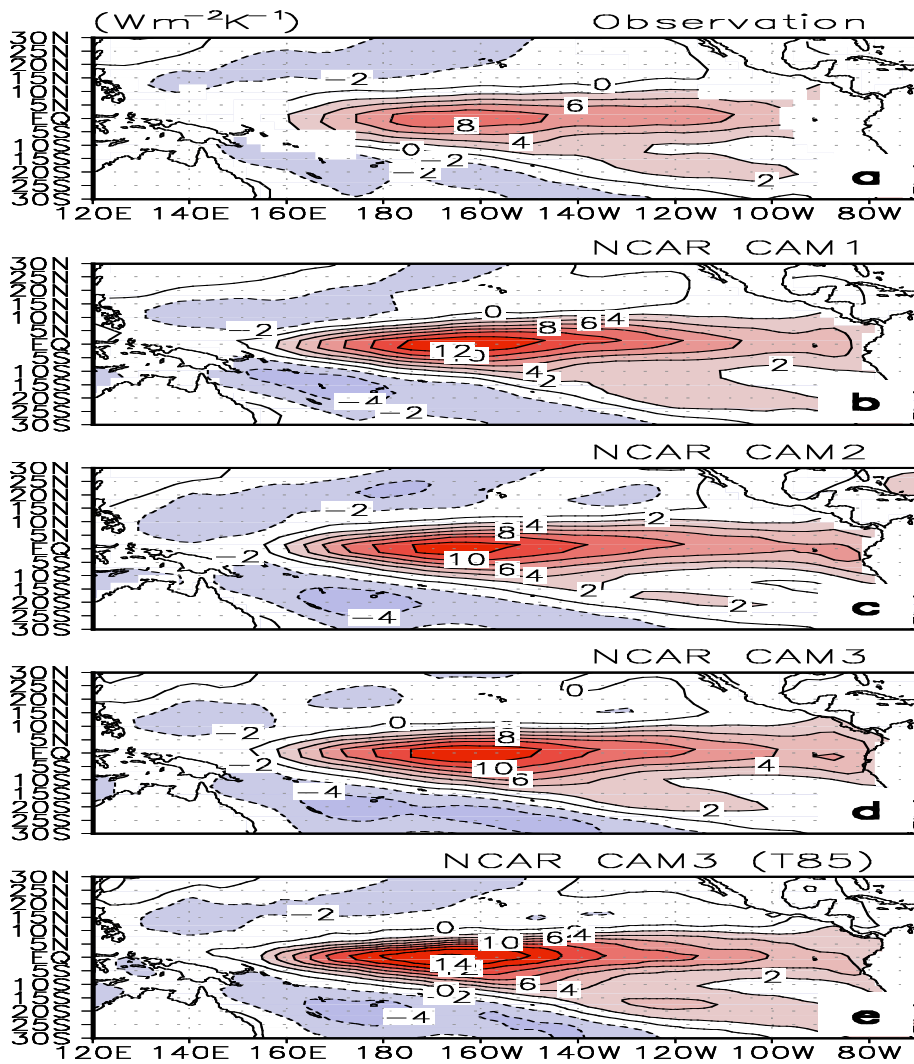


Figure 1: Response of the greenhouse effect of water vapor (G_a) to El Niño warming from (a) ERBE observations, (b) CAM1, (c) CAM2, (d) T42 CAM3, and (e) T85 CAM3. Shown are regression coefficients obtained by linearly regressing the greenhouse effect of water vapor at each grid point against the underlying SST averaged over the region of El Niño warming (160°E - 290°E , 5°S - 5°N). The interannual variations of G_a over the ERBE period are used for the calculations.

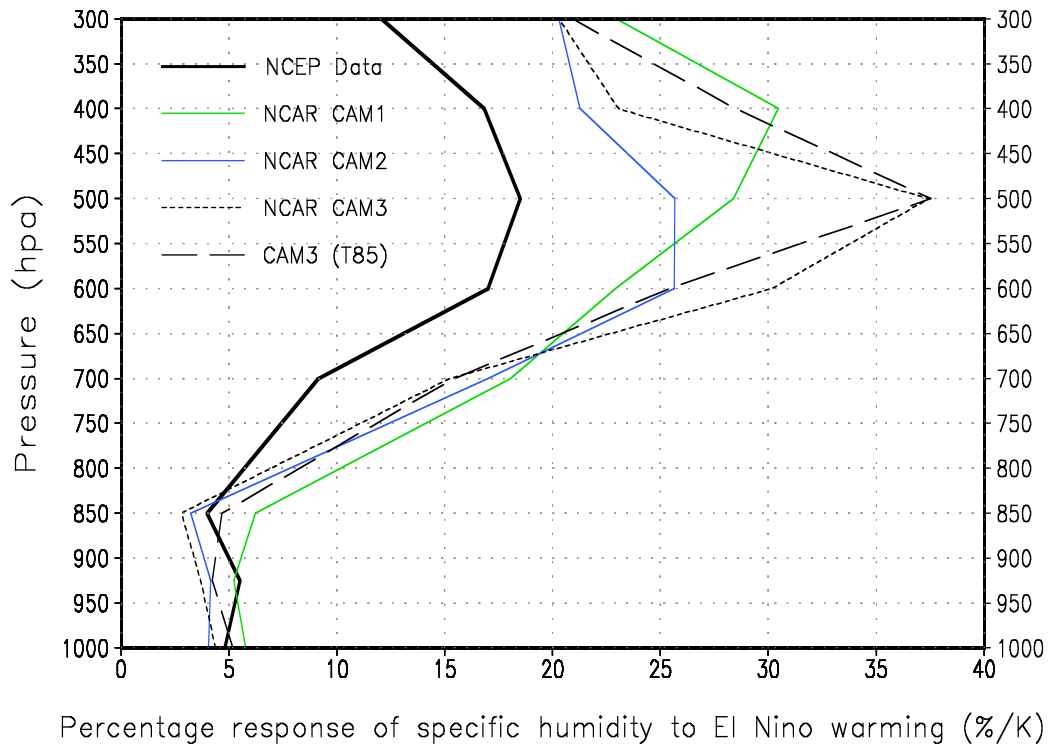


Figure 2: Percentage response of specific humidity to El Niño warming as a function of height from the NCEP-NCAR reanalysis and four NCAR models averaged over the equatorial Pacific (160°E-290°E, 5°S-5°N). Shown are regression coefficients divided by the respective climatology. In every vertical level, the regression coefficients are obtained by linearly regressing specific humidity at the corresponding level against the underlying SST (as in Figure 19 of Zhang and Sun [2006]) averaged over the region of El Niño warming (160°E-290°E, 5°S-5°N). The interannual variations of specific humidity over the ERBE period are used for the regression calculations.

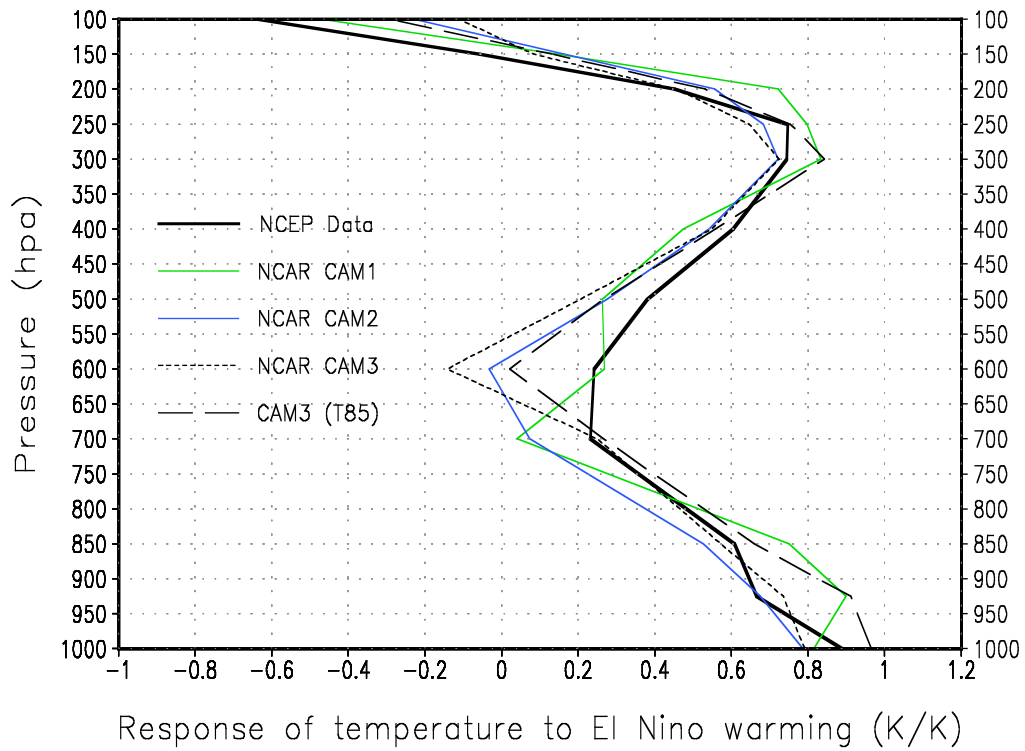


Figure 3: Response of air temperature to El Niño warming as a function of height from the NCEP-NCAR reanalysis and four NCAR models averaged over the equatorial Pacific (160°E-290°E, 5°S-5°N). Shown in every vertical level are regression coefficients obtained by linearly regressing the air temperature at the corresponding level against the underlying SST averaged over the region of El Niño warming (160°E-290°E, 5°S-5°N). The interannual variations of air temperature over the ERBE period are used for the regression calculations.